



## Short communication

## Validation of a novel method for quantifying and comparing regional ACL elongations during uniaxial tensile loading

Mélanie L. Beaulieu<sup>a,\*</sup>, Jeffrey A. Haladik<sup>b</sup>, Michael J. Bey<sup>b</sup>, Scott G. McLean<sup>a</sup><sup>a</sup> School of Kinesiology, University of Michigan, Ann Arbor, MI, USA<sup>b</sup> Bone and Joint Center, Henry Ford Hospital, Detroit, MI, USA

## ARTICLE INFO

## Article history:

Accepted 9 August 2012

## Keywords:

Biomechanics  
Anterior cruciate ligament/injuries  
Elongation  
Photogrammetry/methods  
Method validation

## ABSTRACT

Given the complex three-dimensional (3D) knee joint loading associated with anterior cruciate ligament (ACL) injuries, accurate site- and bundle-specific strain measurements are critical. The purpose of this study was to quantify tensile load-induced migrations of radio-opaque markers injected directly into the ACL, as a first step in validating a roentgen stereophotogrammetric analysis-based method for measuring ligament strain. Small markers were inserted into the femur and tibia, as well as injected into the antero-medial bundle of the ACL of eight (42–56 yrs) femur–ACL–tibia complexes (FATCs). The FATCs were then loaded under tension along the ligament's longitudinal axis by a material testing machine from 10 N to 50 N, 100 N, 125 N, and 150 N, each over 10 load–unload cycles. Complexes were imaged before the loading protocol, between each loading sequence, and after the protocol via biplane radiography. Marker migrations within the ACL tissue were quantified as the difference in their 3D positions between the pre- and each post-loading condition. Negligible migration was evident, with the lowest average root mean square values observed along the longitudinal axis of the ACL, ranging from 0.128 to 0.219 mm. Further, neither marker location nor load magnitude significantly affected migration values. This innovative method, therefore, presents as a plausible means to measure global and regional ACL strains, as small as 0.75% strain. In particular, it may provide important new insights in ACL strain behaviors during complex 3D knee load states associated with ligament injury.

© 2012 Elsevier Ltd. All rights reserved.

## 1. Introduction

The strains experienced by a ligament impact its potential for injury (Woo et al., 1991). Accurate characterization of anterior cruciate ligament (ACL) strain is particularly critical, considering ACL injuries present with significant short- and longer-term morbidities (Griffin et al., 2006). Transducers implanted within (Amis and Dawkins, 1991) or mounted on the ACL (Mizuno et al., 2009) have been used extensively for this purpose, with the differential variable reluctance transducer (DVRT) being the “gold standard”. The DVRT has been used both in vivo and in vitro to gain insights into the mechanisms (Cerulli et al., 2003; Oh et al., 2012) and rehabilitation (Beynon et al., 1995) of ACL injuries. These devices, however, record localized strains only. They cannot capture potentially important regional strain inhomogeneities (Butler et al., 1990) and are not suitable for long-term implantation. Further, their fragility retards assessment of critical interactions between the ACL and surrounding joint anatomies (Fung and Zhang, 2003).

More robust methods that can comprehensively characterize ACL strain responses thus appear imperative.

Roentgen stereophotogrammetric analysis (RSA) methods have been validated to quantify site-specific tibialis tendon allograft length changes under clinical loads. Such changes are quantified by tracking radio-opaque markers injected into the tendon, which demonstrate minimal migration within the tissue over extensive loading cycles (Smith et al., 2005). This innovative approach has not been considered for ACL strain measures. As a critical first step in validating RSA for this purpose, we aimed to quantify migration magnitudes of radio-opaque markers injected directly into the ACL in response to uniaxial tensile loads.

## 2. Methods

The femur–ACL–tibia complex (FATC) of 8 unpaired cadaveric knees (4 males; 4 females; 42–56 years; 25.2–31.4 mm ACL length) were prepared by cutting the femur and tibia parallel to the longitudinal axis of the ACL, as described by Chandrashekar et al. (2006). Each bone plug was then potted in polymethylmethacrylate, with four steel markers (1.98 mm diameter) implanted on their medial/lateral facets (Fig. 1A). Two markers approximated a line parallel to the ACL longitudinal axis when the complex was extended.

\* Corresponding author. Tel.: +1 734 936 0367; fax: +1 734 936 1925.  
E-mail address: mbeaulie@umich.edu (M.L. Beaulieu).

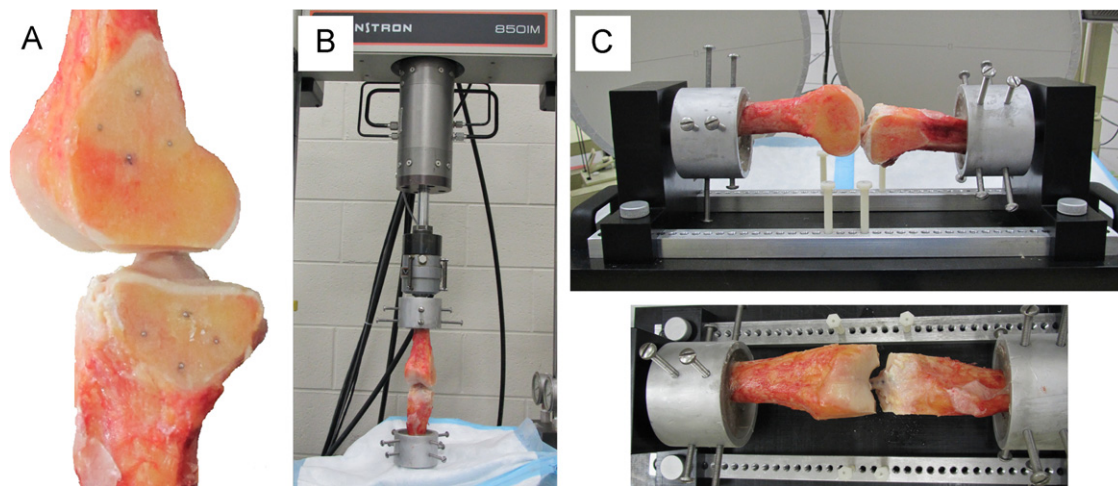


**Fig. 1.** (A) Location of 1.98 mm steel markers embedded within the femoral and tibial bone plugs; (B) FATC potted and mounted in the material testing machine and (C) FATC secured in the custom-built stabilization device located within the field of view of the biplane radiography system.

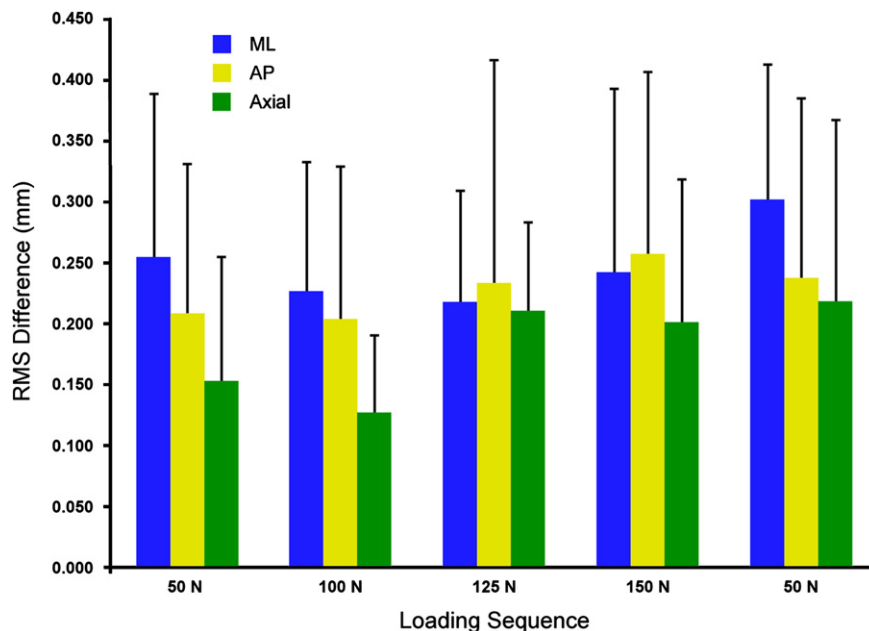


**Fig. 2.** Mean (+SD) RMS differences in injected AMB marker positions relative to baseline (pre-loaded). RMS values are reported along each local femoral coordinate axis. ML=axis parallel to the AMB medio-lateral axis; AP=axis parallel to the AMB antero-posterior axis; Axial=axis parallel to the AMB longitudinal axis.

Once prepared, the FATC was mounted in a material testing machine (8501M, Instron, Norwood, MA, USA) (Fig. 1B), loaded under tension to 10 N, and preconditioned from 10 N to 50 N over 10 load-unload cycles at 0.25 Hz. It was then cyclically loaded (10 cycles) from 10 N to 100 N. The FATC was removed from the machine and five to six brass markers (0.79 mm diameter) were injected into the ACL's antero-medial bundle (AMB) at 5 mm intervals along its length via an 18-gauge needle and at a depth of 3 mm controlled for by constant needle insertion depth. Subsequently, the fully extended complex was fixed within a custom-built stabilization device, which afforded accurate repositioning with the ACL under a small tension load ( $\approx 3$ –4 N), and imaged with a biplane radiography system (Fig. 1C). With the exception of new image intensifiers (TH 9447 QX H404 L, Thales Electron Devices, Cedex, France), this system has been described (Bey et al., 2008). Each imaging sequence comprised three 0.3 s trials collected at 120 Hz.

Following initial imaging, the complex was re-mounted in the material testing machine, loaded under tension to 50 N at 0.25 Hz over 10 load-unload cycles, removed, fixed within the stabilization device, and re-imaged. This loading-imaging sequence was repeated for 100 N, 125 N, 150 N, and an additional 50 N load(s). Load sequences were approximately 8–10 min apart to offset potential ligament creep effects. FATCs were kept hydrated with phosphate buffered solution throughout the experiment.

Using RSA, three-dimensional (3D) coordinates of each marker were determined from their two-dimensional position in each x-ray image with custom software (Tashman and Anderst, 2003). They were averaged across 10 frames for each trial,

and then over the three trials comprising each imaging sequence. A custom Matlab program then transformed the 3D global coordinates of each AMB marker to a local femoral coordinate system via standard rotational and linear transformations. This local coordinate system was defined by the bone embedded markers, whose  $x$ -,  $y$ -, and  $z$ -axes approximated the medio-lateral, antero-posterior, and longitudinal axes of the ACL, respectively. Marker migrations in response to each load sequence were quantified along each femoral axis with respect to their initial (preload) positions.

Friedman tests examined whether marker migration along the AMB longitudinal axis systematically increased with additional loading. Additional Friedman tests determined whether migration magnitudes were sensitive to marker insertion location. Specifically, absolute (longitudinal axis) migrations were compared across markers located (1) nearest the femoral AMB insertion, (2) nearest the tibial AMB insertion, and (3) nearest the AMB mid-substance (middle marker or average of middle two markers). For reporting and graphical purposes, root mean square (RMS) values were computed, representing average ACL marker migration across all markers, and averaged across all specimens.

The FATC repositioning precision within the stabilizing device following each load sequence was calculated as the difference in locally (device) defined 3D femoral marker positions compared to the original (pre-load) state. RMS values, representing average differences across all markers, were calculated and averaged across all load sequences and specimens. In addition, the biplane radiography system's precision was estimated from differences in 3D marker coordinates between trials of each imaging sequence, during which positions were constant.

Stiffness data obtained from the two (pre- and post-marker injection) 100 N load sequences were compared to determine whether ligament structural properties were compromised via the injection method. Force data of the last eight cycles of each load sequence were filtered using a 4th order low-pass Butterworth filter (cut-off frequency of 3 Hz) and averaged. The linear slopes of the force-displacement curves were subsequently determined and compared using a paired Wilcoxon signed-rank test. For all statistical analyses, an alpha of 0.05 denoted significance.

### 3. Results

Markers within the AMB demonstrated negligible migration following each loading condition (Fig. 2). Average RMS migration values were largest medio-laterally (range: 0.218–0.302 mm), and smallest longitudinally (range: 0.128–0.219 mm). Load-induced changes in individual marker positions are presented for a sample specimen (Fig. 3). Changes along the ACL longitudinal axis did not increase as load sequences progressed ( $p=0.258$ – $0.861$  for markers 1–6). Mean marker migrations were also not significantly different when compared across the three AMB regions (Table 1;  $p=0.197$ – $0.882$  for all load sequences (50–150 N)).

The FATCs were repositioned in the stabilization device with mean precision of  $0.102 \pm 0.081$  mm,  $0.158 \pm 0.112$  mm, and  $0.197 \pm 0.135$  mm along its width, height, and length, respectively. The precision of our radiography system was  $0.026 \pm 0.015$  mm and  $0.020 \pm 0.010$  mm for the 0.79 mm and 1.98 mm markers, respectively. Furthermore, ACL stiffness was not significantly different with or without markers in the ligament (Table 2;  $p=0.327$ ).

### 4. Discussion

This study provides support for quantifying ACL strains via (RSA) tracking of radio-opaque markers injected into the ligament. Negligible marker migration within the tissue was evident, particularly longitudinally, when cyclically loaded. Migration magnitudes were not sensitive to insertion location along the ligament's length. Accurate quantification of global and/or regional ACL strains via this method thus seems plausible.

This RSA-based assessment method appears well suited to compare global ACL strains across various scenarios that load the ligament. Strains of 3.6% and 5.47%, for example, have been

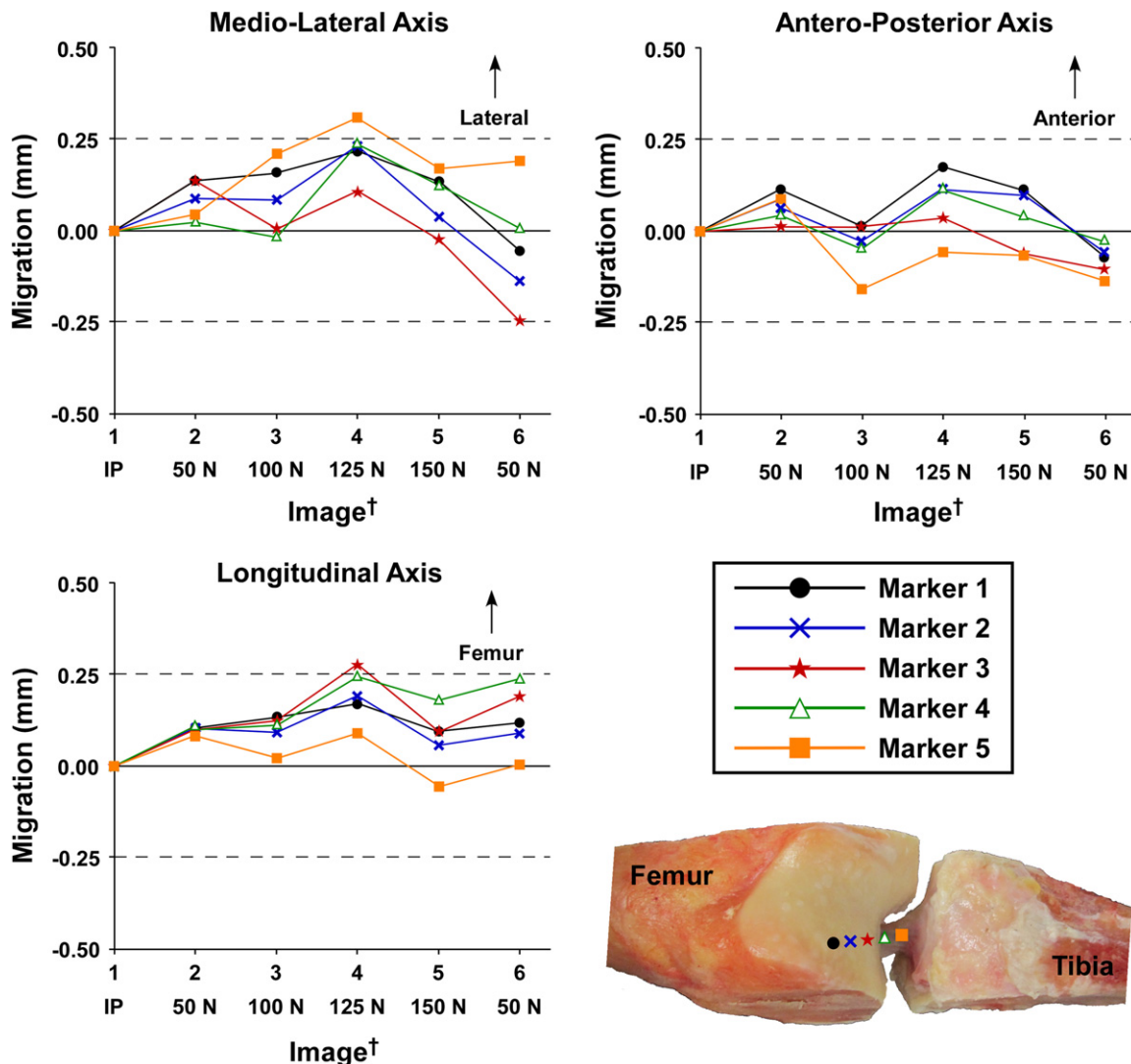


**Fig. 3.** Individual marker migrations relative to baseline (pre-loaded) following each loading sequence for a sample specimen. Marker numbers are in ascending order from femoral to tibial insertion sites. IP: initial position. †Loads below the imaging sequences indicate the load applied to the femur–ACL–tibia complex over 10 cycles prior to that sequence of marker imaging.

**Table 1**  
RMS differences (mm) in 3D marker position across all specimens for three distinct AMB regions following explicit load cycles relative to the baseline (pre-loaded) condition.

Marker location	Image														
	50 N <sup>a</sup>			100 N <sup>a</sup>			125 N <sup>a</sup>			150 N <sup>a</sup>			50 N <sup>a</sup>		
	ML	AP	Axial	ML	AP	Axial	ML	AP	Axial	ML	AP	Axial	ML	AP	Axial
Femur	0.318	0.311	0.196	0.301	0.360	0.230	0.241	0.236	0.317	0.246	0.279	0.257	0.332	0.263	0.357
Mid	0.273	0.197	0.175	0.239	0.177	0.081	0.229	0.286	0.170	0.296	0.251	0.176	0.324	0.268	0.208
Tibia	0.243	0.259	0.204	0.231	0.252	0.106	0.226	0.284	0.208	0.329	0.275	0.197	0.329	0.242	0.224

Femur: data from the marker closest to the femoral insertion site.

Mid: data from the marker(s) in the mid-substance of the AMB (middle marker and average of middle two markers for FATCs with 5 and 6 markers, respectively).

Tibia: data from the marker closest to the tibial insertion site.

ML: migration along the medio-lateral axis of the AMB.

AP: migration along the antero-posterior axis of the AMB.

Axial: migration along the longitudinal axis of the AMB.

<sup>a</sup> Loads applied to the femur-ACL-tibia complex over 10 cycles prior to imaging of markers.

**Table 2**

Specimen-specific linear ACL stiffness, based on average force-displacement curves calculated from eight 100 N load cycles, prior to and following marker insertion into the ligament.

Specimen	Stiffness (N/mm)	
	w/o markers	w/ markers
1	76.99	77.17
2	75.62	75.18
3	104.44	86.96
4	82.06	83.34
5	102.05	100.91
6	119.46	118.82
7	134.36	135.01
8	77.46	75.07

reported during squatting and dynamic deceleration tasks, respectively (Beynon and Fleming, 1998; Cerulli et al., 2003). Elongations measured within an accuracy of 0.219 mm (largest mean marker migration), therefore, will successfully distinguish between length increases that occur during such tasks ( $\approx 0.9$ – $1.1$  mm vs.  $\approx 1.4$ – $1.7$  mm elongations) based on the length of the ACLs included herein. This technique can also successfully detect smaller strains, as small as 0.75%, and thus distinguish between a relatively large range of elongations.

Outcomes also suggest the method may successfully delineate regional ACL strain behaviors. This step seems critical to elucidating ACL injury mechanisms considering the complex 3D joint loads associated with injury likely precipitate an equally complex ligament strain response. The need to avoid contact with surrounding joint structures currently restricts DVRT placement to the distal third of the AMB. By inserting markers directly into the tissue, our method not only affords synchronous strain measures across multiple ligament sites and/or bundles, but also enables joint anatomical effects on these strains to be considered. The method's utility may be compromised, however, if explicit ligament regions demonstrate negligible strain (i.e., within method's uncertainty of  $\pm 0.75\%$  strain).

An RSA-based ACL strain measurement technique is not without drawbacks. First, it requires an imaging system, such as biplane radiography, which is more expensive and methodologically complex than a DVRT. Second, inserting markers directly into ACL may compromise tissue integrity, although our comparable ACL stiffness data suggests otherwise. All but one of the FATCs experienced negligible changes in stiffness (Table 2). It is unclear, however, whether specimen 3 is an outlier or represents a subgroup affected by marker injection. Third, in vivo application

may be limited given the associated radiation levels and limited ability to remove ligament markers post-examination. If valid in vivo techniques can be developed (Smith et al., 2010), however, then complex long-term ACL strain assessments may be possible.

Study outcomes should be considered in light of several limitations. Marker migration was quantified in response to uniaxial tensile loading only although the ACL most likely undergoes shear loading as well. Also, it was not possible to establish whether marker migrations were due to (1) the markers moving relative to the collagen fibrils or (2) actual load-induced fibril movement. We assumed it was the former, worst-case scenario, and thus calculated a conservative estimate of this technique's accuracy. If marker migration did arise via the latter, we underestimated therefore this technique's accuracy. Furthermore, since we could not image the FATC while mounted in the material testing machine, inconsistent FATC repositioning may have confounded migration measurements. Data strongly suggest, however, that FATCs were positioned with high accuracy.

## 5. Conflict of interest statement

The authors have no conflict of interest to declare.

## Acknowledgments

The authors would like to acknowledge Richard Banglmaier for his contribution to the design of the loading protocol.

## References

- Amis, A.A., Dawkins, G.P., 1991. Functional anatomy of the anterior cruciate ligament. Fibre bundle actions related to ligament replacements and injuries. *Journal of Bone and Joint Surgery British* 73, 260–267.
- Bey, M.J., Kline, S.K., Zauel, R., Lock, T.R., Kolowich, P.A., 2008. Measuring dynamic in-vivo glenohumeral joint kinematics: technique and preliminary results. *Journal of Biomechanics* 41, 711–714.
- Beynon, B.D., Fleming, B.C., 1998. Anterior cruciate ligament strain in-vivo: a review of previous work. *Journal of Biomechanics* 31, 519–525.
- Beynon, B.D., Fleming, B.C., Johnson, R.J., Nichols, C.E., Renstrom, P.A., Pope, M.H., 1995. Anterior cruciate ligament strain behavior during rehabilitation exercises in vivo. *American Journal of Sports Medicine* 23, 24–34.
- Butler, D.L., Sheh, M.Y., Stouffer, D.C., Samaranyake, V.A., Levy, M.S., 1990. Surface strain variation in human patellar tendon and knee cruciate ligaments. *Journal of Biomechanical Engineering* 112, 38–45.
- Cerulli, G., Benoit, D.L., Lamontagne, M., Caraffa, A., Liti, A., 2003. In vivo anterior cruciate ligament strain behaviour during a rapid deceleration movement: case report. *Knee Surgery Sports Traumatology Arthroscopy* 11, 307–311.

- Chandrashekar, N., Mansouri, H., Slauterbeck, J., Hashemi, J., 2006. Sex-based differences in the tensile properties of the human anterior cruciate ligament. *Journal of Biomechanics* 39, 2943–2950.
- Fung, D.T., Zhang, L.Q., 2003. Modeling of ACL impingement against the intercondylar notch. *Clinical Biomechanics* 18, 933–941.
- Griffin, L.Y., Albohm, M.J., Arendt, E.A., Bahr, R., Beynon, B.D., Demaio, M., Dick, R.W., Engebretsen, L., Garrett Jr., W.E., Hannafin, J.A., Hewett, T.E., Huston, L.J., Ireland, M.L., Johnson, R.J., Lephart, S., Mandelbaum, B.R., Mann, B.J., Marks, P.H., Marshall, S.W., Myklebust, G., Noyes, F.R., Powers, C., Shields Jr., C., Shultz, S.J., Silvers, H., Slauterbeck, J., Taylor, D.C., Teitz, C.C., Wojtys, E.M., Yu, B., 2006. Understanding and preventing noncontact anterior cruciate ligament injuries: a review of the Hunt Valley II meeting, January 2005. *American Journal of Sports Medicine* 34, 1512–1532.
- Mizuno, K., Andrich, J.T., van den Bogert, A.J., McLean, S.G., 2009. Gender dimorphic ACL strain in response to combined dynamic 3D knee joint loading: implications for ACL injury risk. *Knee* 16, 432–440.
- Oh, Y.K., Lipps, D.B., Ashton-Miller, J.A., Wojtys, E.M., 2012. What strains the anterior cruciate ligament during a pivot landing? *American Journal of Sports Medicine* 40, 574–583.
- Smith, C.K., Hull, M.L., Howell, S.M., 2005. Migration of radio-opaque markers injected into tendon grafts: a study using roentgen stereophotogrammetric analysis (RSA). *Journal of Biomechanical Engineering* 127, 887–890.
- Smith, C.K., Hull, M.L., Howell, S.M., 2010. Does graft construct lengthening at the fixations cause an increase in anterior laxity following anterior cruciate ligament reconstruction in vivo? *Journal of Biomechanical Engineering* 132, 081001.
- Tashman, S., Anderst, W., 2003. In-vivo measurement of dynamic joint motion using high speed biplane radiography and CT: application to canine ACL deficiency. *Journal of Biomechanical Engineering* 125, 238–245.
- Woo, S.L., Hollis, J.M., Adams, D.J., Lyon, R.M., Takai, S., 1991. Tensile properties of the human femur–anterior cruciate ligament–tibia complex. The effects of specimen age and orientation. *American Journal of Sports Medicine* 19, 217–225.